AIAA AVIATION Forum
17-21 June 2019, Dallas, Texas
AIAA Aviation 2019 Forum

10.2514/6.2019-3707

Transform & Learn: A data-driven approach to nonlinear model reduction

Elizabeth Y. Qian*, Boris Kramer†, and Alexandre Marques‡
Massachusetts Institute of Technology, Cambridge, Massachusetts 02139

Karen E. Willcox§
University of Texas at Austin, Austin, Texas 78712

This paper presents *Transform & Learn*, a physics-informed surrogate modeling approach that unites the perspectives of model reduction and machine learning. The proposed method uses insight from the physics of the problem—in the form of partial differential equation (PDE) models—to derive a state transformation in which the system admits a quadratic representation. Snapshot data from a high-fidelity model simulation are transformed to the new state representation and subsequently are projected onto a low-dimensional basis. The quadratic reduced model is then learned via a least-squares-based operator inference procedure. The state transformation thus plays two key roles in the proposed method: it allows the task of nonlinear model reduction to be reformulated as a structured model learning problem, and it parametrizes the machine learning problem in a way that recovers efficient, generalizable models. The proposed method is demonstrated on two PDE examples. First, we transform the Euler equations in conservative variables to the specific volume state representation, yielding low-dimensional Transform & Learn models that achieve a 0.05% relative state error when compared to a high-fidelity simulation in the conservative variables. Second, we consider a model of the Continuously Variable Resonance Combustor, a single element liquid-fueled rocket engine experiment. We show that the specific volume representation of this model also has quadratic structure and that the learned quadratic reduced models can accurately predict the growing oscillations of an unstable combustor.

I. Nomenclature

A	=	cross-sectional area
$\mathbf{A}$, $\hat{\mathbf{A}}$	=	full and reduced linear operator matrices for linear-quadratic ODE
C_{fo}	=	fuel-oxidizer ratio
E	=	total energy
$\mathbf{F}$	=	nonlinear function describing ODE state evolution
$\mathbf{H}$, $\hat{\mathbf{H}}$	=	full and reduced matricized quadratic tensor operators for linear-quadratic ODE
K	=	number of state snapshots used to compute POD basis
$\dot{m}_f$	=	fuel mass flow rate
N	=	full state dimension
r	=	reduced state dimension
$\mathbf{s}$, $\hat{\mathbf{s}}$	=	full and reduced system states for general nonlinear ODE
$\mathbf{S}$	=	snapshot matrix containing snapshots of general nonlinear state
t	=	time
u	=	velocity
$\mathbf{U}_{1:r}$	=	POD basis of dimension r
p	=	pressure
$\mathbf{w}$, $\hat{\mathbf{w}}$	=	full and reduced system states for linear-quadratic ODE

*Graduate student, Department of Aeronautics & Astronautics, elizqian@mit.edu, Member AIAA.
†Postdoctoral Associate, Department of Aeronautics & Astronautics, bokramer@mit.edu.
‡Postdoctoral Associate, Department of Aeronautics & Astronautics, noll@mit.edu.
§Professor of Aerospace Engineering and Engineering Mechanics, kwillcox@oden.utexas.edu, Fellow AIAA.

$\mathbf{W}, \dot{\mathbf{W}}$	=	snapshot and time derivative data matrices for linear-quadratic state
α	=	unsteady heat release parameter
Δh_0	=	heat of reaction
Δx	=	mesh size
γ	=	heat capacity ratio
ρ	=	density
ρu	=	specific momentum
$\dot{\omega}_f$	=	fuel injection source term
ζ	=	specific volume, $\zeta = \frac{1}{\rho}$
$\otimes$	=	Kronecker product

II. Introduction

This paper proposes a new surrogate modeling approach that unites advantages from two approaches to nonlinear system approximation: projection-based model reduction and machine learning. The development of inexpensive surrogate models is a critical enabling technology for many-query computations such as optimization, uncertainty quantification, and control. In these settings, a predictive simulation of the system must be evaluated many times, so traditional simulation methods based on high-dimensional spatial discretizations of nonlinear partial differential equations (PDEs) can be prohibitively expensive. In our approach, we use physics information from the governing PDEs to formulate a structured learning problem which recovers accurate, analyzable reduced-order models.

Projection-based model reduction starts with a high-dimensional full-order model (FOM), and obtains the reduced-order model (ROM) by projecting the FOM equations onto a low-dimensional subspace. When the FOM has polynomial structure, projecting the FOM onto the reduced space yields low-dimensional matrix operators that preserve the polynomial structure of the FOM [1–5]. This preservation of polynomial structure means that the ROM may then be cheaply evaluated many times, with a cost independent of the FOM dimension. For linear systems, the preservation of structure also enables the derivation of rigorous error estimators for the ROM [6–9]. For nonlinear PDEs without polynomial structure, however, simulating the ROM is expensive because it requires reconstruction of the high-dimensional state. To recover computational efficiency, state-of-the-art methods [8, 10–15] evaluate the nonlinear term at only selected elements of the state and interpolate. These methods sacrifice structure, making analysis of the resultant ROM more difficult. Additionally, for some problems the number of interpolation points required for accuracy limits the achievable speedups [16, 17].

In contrast to the intrusive nature of projection-based model reduction, where users must have access to the high-dimensional operators, machine learning methods treat the PDE simulation as a black box. These methods seek only to approximate an input-output mapping based on data. The parametrization of this mapping is critical to the efficiency and accuracy of the learned model [18, 19]. Neural networks provide a general architecture that can accurately approximate a large class of functions [20], but the amount of data required to accurately train them presents a barrier to their use when the data comes from large-scale PDE simulations [21], they struggle to generalize to regimes outside of their training data, and rigorous error analysis remains a challenge. To obtain generalizable and analyzable models, a different body of work uses techniques from compressive sensing to identify the true terms of a governing equation from a large library of candidate terms [19, 22, 23]. When the form of the model is known exactly, then the learning problem can be formulated as a parameter estimation. In the work in [24], on which we build, data is used to learn matrix operators for large systems of ordinary differential equations (ODEs) with polynomial nonlinearities in the state.

Knowledge of polynomial structure in the nonlinear model thus presents advantages in both learning and model reduction approaches. Variable transformations allow the benefits of structure to be exploited even when the original model has no such structure: for example, the work in [3, 25] exploits lifting transformations to quadratic form for model reduction. In this paper, by transforming the PDE state to a representation in which the PDE has polynomial structure, we can reformulate the nonlinear model reduction task as a structured model learning problem, with the accompanying benefits of non-intrusivity and avoiding cumbersome interpolation procedures. Likewise, transformation to a representation with polynomial structure enables the learning problem to be efficiently formulated, leading to models that generalize well to regimes outside their training data and which are amenable to error and stability analysis.

Section III presents necessary background on model reduction, learning polynomial models, and variable transformations. In Section IV we present the Transform & Learn method. Section V presents results on the Euler equations and on a combustion example.

III. Background

In this section, we present background in nonlinear model reduction (Section III.A), learning polynomial models (Section III.B), and variable transformations (Section III.C).

A. Nonlinear model reduction via proper orthogonal decomposition

Proper orthogonal decomposition (POD) [26, 27] is the most widely-used method for nonlinear model reduction, and has been successfully applied in aerodynamic applications [28–35]. We present POD here for an N-dimensional system of ODEs of the form

$$\frac{\mathrm{d}\mathbf{s}}{\mathrm{d}t} = \mathbf{F}(\mathbf{s}), \tag{1}$$

where $\mathbf{s} \in \mathbb{R}^N$ is the state, and the nonlinear function $\mathbf{F} : \mathbb{R}^N \mapsto \mathbb{R}^N$ maps the state to its time derivative. In applications where the underlying model is a PDE, N is typically large. In POD, the full system is simulated and the state is recorded at K time instances t_i, for $i = 1, \ldots, K$. These state snapshots are collected and used to compute a reduced basis onto which the operators of the full system are projected. Let the snapshot data matrix $\mathbf{S} \in \mathbb{R}^{N\times K}$ be given by

$$\mathbf{S} = \begin{pmatrix} | & | & & | \\ \mathbf{s}(t_0) & \mathbf{s}(t_1) & \cdots & \mathbf{s}(t_K) \\ | & | & & | \end{pmatrix}. \tag{2}$$

The singular value decomposition of $\mathbf{S}$ is given by $\mathbf{S} = \mathbf{U}\Sigma\mathbf{V}^\top$, and the POD basis of size r, denoted $\mathbf{U}_{1:r}$, consists of the first r columns of $\mathbf{U}$. The state $\mathbf{s}$ is then approximated in the POD subspace spanned by the first r POD basis functions as

$$\mathbf{s} \approx \mathbf{U}_{1:r}\hat{\mathbf{s}}, \tag{3}$$

where $\hat{\mathbf{s}}$ is the r-dimensional reduced state. By substituting Eq. 3 into Eq. 1 and applying the standard Galerkin projection, we obtain the following r-dimensional POD ROM:

$$\frac{\mathrm{d}\hat{\mathbf{s}}}{\mathrm{d}t} = \mathbf{U}_{1:r}^\top \mathbf{F}(\mathbf{U}_{1:r}\hat{\mathbf{s}}). \tag{4}$$

For general $\mathbf{F}(\cdot)$, the cost of evaluating Eq. 4 scales not with r but with N. To achieve reductions in computational cost, an additional reduction step must be taken, e.g., by evaluating $\mathbf{F}(\cdot)$ at only a subset of the elements of $\mathbf{U}_{1:r}\hat{\mathbf{s}}$ and interpolating. This is often referred to as hyper-reduction. Several methods for doing this have been proposed in [8, 10–14]. While this is often successful, applications in combustion systems have shown [16, 36] that due to the complexity of reacting flows, a large number of interpolation points is needed, effectively eliminating the ROM computational savings. Moreover, subsampling procedures used in hyper-reduction are in general not amenable to rigorous analysis of ROM properties such as stability and errors.

However, if $\mathbf{F}(\cdot)$ has polynomial structure, the reduced-order model preserves this structure. Consider a linear-quadratic FOM of the form

$$\frac{\mathrm{d}\mathbf{w}}{\mathrm{d}t} = \mathbf{F}(\mathbf{w}) = \mathbf{A}\mathbf{w} + \mathbf{H}(\mathbf{w} \otimes \mathbf{w}), \tag{5}$$

where $\mathbf{A} \in \mathbb{R}^{N\times N}$, $\mathbf{H} \in \mathbb{R}^{N\times N^2}$ are matrix operators and $\otimes$ denotes the Kronecker product for vectors. Here, and in the remainder of the paper, $\mathbf{w}$ is used to denote states that have linear-quadratic evolution, and $\mathbf{s}$ is used to denote states described by general nonlinear equations. Then, substituting Eq. 3 into Eq. 5 and applying the standard Galerkin approximation yields the following linear-quadratic POD ROM:

$$\frac{\mathrm{d}\hat{\mathbf{w}}}{\mathrm{d}t} = \hat{\mathbf{A}}\hat{\mathbf{w}} + \hat{\mathbf{H}}(\hat{\mathbf{w}} \otimes \hat{\mathbf{w}}), \tag{6}$$

where the reduced operators are given by $\hat{\mathbf{A}} = \mathbf{U}_{1:r}^\top \mathbf{A}\mathbf{U}_{1:r}$ and $\hat{\mathbf{H}} = \mathbf{U}_{1:r}^\top \mathbf{H}(\mathbf{U}_{1:r} \otimes \mathbf{U}_{1:r})$. The reduced operators $\hat{\mathbf{A}}$ and $\hat{\mathbf{H}}$ can be pre-computed, allowing evaluations of Eq. 6 to be computed cheaply. This avoids the need to approximate the nonlinear term through hyper-reduction, and thus retains some hope for analysis of the reduced system.

B. Polynomial operator inference

In this subsection, we present the polynomial operator inference framework developed in [24]. We consider again a linear-quadratic system of ODEs, as in Eq. 5. If a model is known to have the form in Eq. 5, but the actual coefficients contained in $\mathbf{A}$ and $\mathbf{H}$ are unknown, a natural approach is to learn the matrix operators from state and time derivative data. We collect state snapshots taken at times $t_1, \ldots, t_K$, as well as the corresponding state time derivative data. We define the snapshot and time derivative data matrices, respectively, as

$$\mathbf{W} = \begin{bmatrix} | & & | \\ \mathbf{w}(t_1) & \cdots & \mathbf{w}(t_K) \\ | & & | \end{bmatrix}, \qquad \dot{\mathbf{W}} = \begin{bmatrix} | & & | \\ \dot{\mathbf{w}}(t_1) & \cdots & \dot{\mathbf{w}}(t_K) \\ | & & | \end{bmatrix}. \tag{7}$$

We note that when Eq. 5 arises from the high-dimensional discretization of a quadratic PDE, the operators are high-dimensional and sparse, and can be learned e.g., using the approach in [23]. However, since we are ultimately interested in an efficient low-dimensional model, we present the approach of [24] here.

Let $\mathbf{U}_{1:r}$ be an r-dimensional POD basis for the snapshots collected in $\mathbf{W}$. We project the state and time derivative data onto the space spanned by $\mathbf{U}_{1:r}$ to obtain data for the reduced state and time derivative as follows:

$$\hat{\mathbf{W}} = \mathbf{U}_{1:r}^\top \mathbf{W}, \quad \text{and} \quad \dot{\hat{\mathbf{W}}} = \mathbf{U}_{1:r}^\top \dot{\mathbf{W}}. \tag{8}$$

Since we know the FOM has the form in Eq. 5, we postulate that the reduced state data satisfies the linear-quadratic Galerkin reduced model in Eq. 6. When $\mathbf{A}$ and $\mathbf{H}$ are unknown, $\hat{\mathbf{A}}$ and $\hat{\mathbf{H}}$ cannot be obtained through projection as in Section III.A but must be inferred from data. The least-squares operator inference minimization is given by

$$\min_{\hat{\mathbf{A}} \in \mathbb{R}^{r \times r}, \hat{\mathbf{H}} \in \mathbb{R}^{r \times r^2}} \left\| \hat{\mathbf{W}}^\top \hat{\mathbf{A}}^\top + \left(\hat{\mathbf{W}} \widehat{\otimes} \hat{\mathbf{W}} \right)^\top \hat{\mathbf{H}}^\top - \dot{\hat{\mathbf{W}}}^\top \right\|_F^2, \tag{9}$$

where $\hat{\mathbf{W}} \widehat{\otimes} \hat{\mathbf{W}}$ denotes the matrix whose kth column is given by $\mathbf{w}(t_k) \otimes \mathbf{w}(t_k)$. In Eq. 9, each column of $\hat{\mathbf{W}}^\top$, $\dot{\hat{\mathbf{W}}}^\top$, and $(\hat{\mathbf{W}} \widehat{\otimes} \hat{\mathbf{W}})^\top$ corresponds to the evolution of a single component of the state $\hat{\mathbf{w}}(t)$, leading to r independent least-squares problems (each defined by a column of $\dot{\hat{\mathbf{W}}}^\top$) which can be efficiently solved. The work in [24] shows that as $r \to N$, the inferred operators will converge to the Galerkin ROM operators (Eq. 6).

C. Variable transformations

Variable transformations can elucidate polynomial structure in nonlinear systems. For example, the well-known Cole-Hopf transformation turns the nonlinear Burgers PDE into a linear PDE [37, 38]. In fluid dynamics problems, writing the governing PDEs in specific volume variables rather than the typical conservative variables yields quadratic structure in the PDEs. In this section, we present the specific volume transformation for the Euler equations as well as for a combustor model. Before we proceed, we emphasize that these transformations are exact at the PDE level*; the transformation exactly preserves the physics inherent in the original conservative representation. We also emphasize that our intent is *not* to discretize the transformed systems. Rather, this reformulation at the PDE level identifies a set of features (i.e., the transformed variables) in which the governing equations admit a quadratic formulation. In the next section, we will exploit this fact to learn a quadratic reduced model from data.

1. *Specfic volume transformation of the Euler equations*

The one-dimensional Euler equations are most commonly formulated in the conservative variables,

$$\frac{\partial}{\partial t} \begin{pmatrix} \rho \\ \rho u \\ E \end{pmatrix} = -\frac{\partial}{\partial x} \begin{pmatrix} \rho u \\ \rho u^2 + p \\ (E + p)u \end{pmatrix}, \tag{10}$$

where the state variables are the density ρ, specific momentum ρu, and total energy E, and the equation of state $E = \frac{p}{\gamma - 1} + \frac{1}{2}\rho u^2$ relates energy and pressure via the heat capacity ratio γ. The right-hand side of Eq. 10 contains several

*Note that when considering these transformations we work with the strong form of the equations, which presumes the existence of the derivatives. The presence of discontinuities complicates the situation, but is not considered here.

nonlinear terms that are not quadratic in the chosen state representation. However, the one-dimensional Euler equations can be alternatively formulated in the specific volume variables:

$$\frac{\partial u}{\partial t} = -u\frac{\partial u}{\partial x} - \zeta\frac{\partial p}{\partial x}, \tag{11a}$$

$$\frac{\partial p}{\partial t} = -\gamma p\frac{\partial u}{\partial x} - \frac{\partial p}{\partial x}, \tag{11b}$$

$$\frac{\partial \zeta}{\partial t} = -u\frac{\partial \zeta}{\partial x} + \zeta\frac{\partial u}{\partial x}. \tag{11c}$$

where $\zeta = \frac{1}{\rho}$ is the specific volume, and the other state variables are velocity and pressure. For constant γ, Eq. 11 contains only quadratic nonlinear dependencies on the state and its spatial derivatives. Note that Eq. 11 can be extended to the 3D Euler setting by adding the y- and z-velocity equations.

2. Continuously Variable Resonance Combustor (CVRC) model

The continuously variable resonance combustor (CVRC) is an experiment at Purdue University which has been extensively studied both experimentally [39–41] and computationally [42–45], and is therefore a good candidate for validation of new methods. In this work we use a quasi-1D Euler model for the CVRC [46, 47]:

$$\frac{\partial}{\partial t}\begin{pmatrix}\rho\\ \rho u\\ E\\ \rho Y_{\text{ox}}\end{pmatrix} + \frac{1}{A}\frac{\partial}{\partial x}\begin{pmatrix}A\rho u\\ A(\rho u^2+p)\\ Au(E+p)\\ A\rho u Y_{\text{ox}}\end{pmatrix} = \begin{pmatrix}\dot{\omega}_f\\ \frac{p}{A}\frac{\mathrm{d}A}{\mathrm{d}x} + \dot{\omega}_f u\\ \dot{\omega}_f \Delta h_0\left(1+\alpha\frac{p(x,t-\tau)-\bar{p}(x)}{\bar{p}(x)}\right)\\ -\dot{\omega}_f/C_{fo}\end{pmatrix}, \tag{12}$$

where the conservative state variables are the same as those in the Euler equations, with the addition of ρY_{ox}, where Y_{ox} denotes the oxidizer mass fraction. In the source terms of Eq. 12, which model the chemical reaction and the cross-sectional area variation, α is the unsteady heat release parameter, Δh_0 denotes the heat of reaction, and C_{fo} is the fuel-oxidizer ratio, all of which are constants. Moreover, $A = A(x)$ is a known function that encodes the cross-sectional area of the combustor, $\dot{\omega}_f(x, \dot{m}_f)$ is also a known function of x for fixed fuel mass flow rate $\dot{m}_f$, and $\bar{p}(x)$ is the pressure of the steady solution. The unsteady heat release term depends on the pressure at a previous time $p(t-\tau)$, where the time delay parameter τ can be tuned to match experimental results. For our transformation, we let $\tau = 0$ and model γ as a constant.

As in the 1D Euler equations, the CVRC governing equations admit a quadratic representation when formulated in the specific volume variables:

$$\frac{\partial}{\partial t}\begin{pmatrix}u\\ p\\ \zeta\\ Y_{\text{ox}}\end{pmatrix} = \underbrace{\begin{pmatrix}0\\ (\gamma-1)\dot{\omega}_f\Delta h_0\alpha\frac{p}{\bar{p}(x)}\\ 0\\ -\dot{\omega}_f\frac{1}{C_{fo}}\zeta\end{pmatrix}}_{\text{linear}} + \underbrace{\begin{pmatrix}-u\frac{\partial u}{\partial x} - \zeta\frac{\partial p}{\partial x}\\ -\gamma p\frac{\partial u}{\partial x} - u\frac{\partial p}{\partial x} - \frac{\gamma p u}{A}\frac{\mathrm{d}A}{\mathrm{d}x} - \frac{\gamma-1}{2}u^2\dot{\omega}_f\\ -u\frac{\partial \zeta}{\partial x} + \zeta\frac{\partial u}{\partial x} + \frac{1}{A}\frac{\mathrm{d}A}{\mathrm{d}x}\zeta u - \dot{\omega}_f\zeta^2\\ -u\frac{\partial Y_{\text{ox}}}{\partial x} - \dot{\omega}_f\zeta Y_{\text{ox}}\end{pmatrix}}_{\text{quadratic}} + \underbrace{\begin{pmatrix}0\\ (\gamma-1)(1-\alpha)\dot{\omega}_f\Delta h_0\\ 0\\ 0\end{pmatrix}}_{\text{constant}}. \tag{13}$$

We note that the first term on the right-hand side of Eq. 13 contains terms that are linear in their state dependence; the second term contains terms that have quadratic state dependence, and the third term is state-independent.

IV. Transform & Learn

We now present our Transform & Learn method for learning efficient, generalizable reduced models from data. The steps of our method are as follows:

1) **Perform paper-and-pen transformation of the PDEs to obtain a state representation in which the system admits a quadratic representation.** Examples of such transformations are given in Section III.C. This transformation at the PDE level identifies a set of features, i.e., the transformed variables, for which a quadratic model can be learned.
2) **Obtain state snapshot data (Eq. 2) and corresponding time derivative data by simulating the original system.** We emphasize that in this step, we use existing simulation code for the original equations (Eq. 1). This

code is treated as a black box, and we obtain data in the original variable representation. We do *not* intrusively transform code to produce data in the transformed variables, nor do we discretize the transformed equations.

3) **Transform state and time derivative data to obtain transformed data matrices (Eq. 7).** Using the transformation identified in Step 1, we transform the data collected in Step 2. We postulate that the transformed data can be described by a quadratic model of the form in Eq. 5.
4) **Compute POD basis in the transformed state and obtain projected transformed data (Eq. 8).** By projecting the transformed data onto a POD basis of lower dimension, we obtain data for a reduced state, which can be described by a reduced-order model of the form in Eq. 6.
5) **Solve least-squares minimization (Eq. 9) to obtain reduced linear and quadratic operators in the transformed state.** Because the operators $\hat{\mathbf{A}}$ and $\hat{\mathbf{H}}$ in our proposed ROM are unknown, we use the operator inference approach of [24] to learn the matrix operators from the reduced data obtained in Step 4.

We note that our method relies on the existence of a state transformation for which the transformed PDE contains only quadratic nonlinearities in the state and its time derivatives. Transformation to the specific volume representation achieves this structure for the three-dimensional Euler and Navier-Stokes equations, which underlie a large class of fluid dynamics applications in aerospace settings, in addition to other applications in areas such as hydro- and hemodynamics. Additionally, we have shown in Section III.C.2 an example of such a transformation for equations for reacting flow.

V. Numerical experiments

We apply our Transform & Learn approach to the Euler and CVRC equations from section III.C.

A. Euler equations

We solve Eq. 10 on the periodic domain $x \in [0, 2)$ with mesh size $\Delta x = 0.01$. The initial pressure is set to 1 bar everywhere in the domain. The initial density is a periodic cubic spline interpolation at the points $x = 0, \frac{2}{3}, \frac{4}{3}$, where the interpolation values are drawn from a normal distribution with mean density 22 kg/m^3 and standard deviation 1 kg/m^3. The initial velocity is also a periodic cubic spline interpolation of data at the same x-locations with interpolation values drawn from a normal distribution with mean velocity 100 m/s and standard deviation 5 m/s. Twenty random smooth initial conditions are generated in this way and simulated from $t = 0$ to $t = 0.01$. The resultant trajectories are used to train the Transform & Learn model. Twenty additional random initial conditions are used to generate trajectories for a test set.

The POD basis is computed from the training data set only and the projected training data is used to train the Transform & Learn models. We apply our Transform & Learn framework to infer a quadratic reduced operator $\hat{\mathbf{H}}$ for this system. Note that the transformed system in Eq. 11 contains no linear dependencies on the state, so in our postulated polynomial ROM (Eq. 6), we have $\hat{\mathbf{A}} = 0$. Because the condition number of the least squares data matrix grows rapidly as the basis size is increased, we apply a Tikhonov regularization penalty with weight 0.001 to improve the conditioning of the data matrix. The learned model is then used to simulate the system for each of the 20 initial conditions in the training set and each of the 20 initial conditions in the test set. The average relative reconstruction error over the training and test sets are calculated relative to the $N = 600$-dimensional FOM in conservative variables.

The experiment described above is repeated 20 times; i.e., 20 different sets of random training data are generated, 20 different models are learned from the data, and the learned models are tested on 20 different random test sets. From the 20 experiments, the median, minimum and maximum average errors over the training and test sets are shown in Fig. 1.

For POD basis sizes $r \geq 25$, the Transform & Learn models are stable, accurate, and generalizable, achieving an error under 0.01% for reconstructing the training data and an error under 0.05% for the test data set. For smaller basis sizes, the error in the learned models is higher, and for $r = 10$, the learned models yield unstable trajectories in many of the training data cases and all of the test data cases. This indicates that 10 basis functions are not sufficient to accurately capture the dynamics of the system. A stronger regularization penalty can be used to achieve stable models at this basis size, although this will increase the bias in the model error.

The performance of an intrusive ROM based on a discretization in the specific volume variables is shown for reference. When the basis is rich enough, our Transform & Learn approach achieves a similar error to the intrusive ROM. For the training data, the learned ROMs are in fact slightly more accurate than the intrusive ROMs, as can be seen in the left plot of Fig. 1. However, as the right plot shows, this comes at the expense of a slightly higher error when generalizing to test data. These results highlight the important point of having a sufficiently rich set of training data

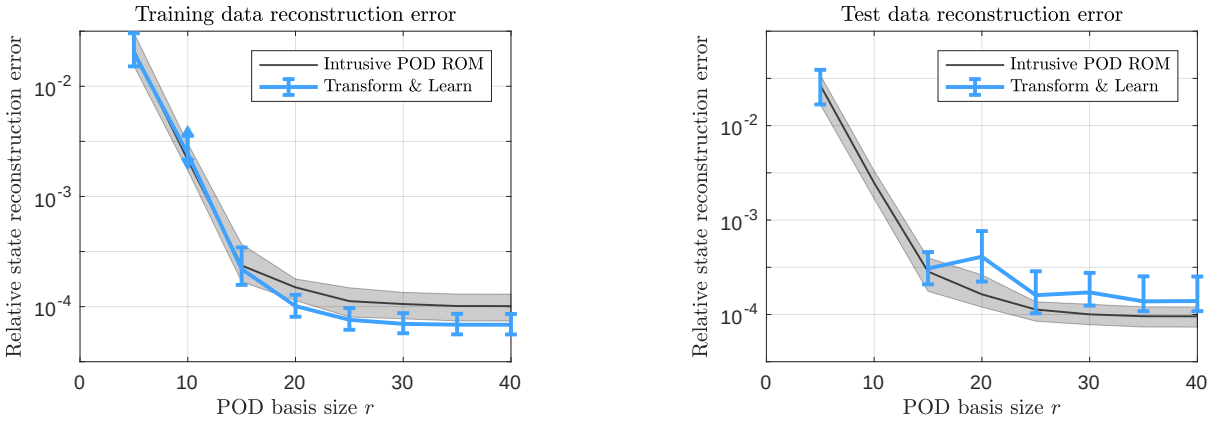

Fig. 1 State reconstruction error of learned ROM in specific volume representation relative to FOM in conservative variables. Minimum and maximum errors over the 20 experiments are shown by the shaded grey region for the intrusive ROM and by the error bars for the Transform & Learn model.

to avoid overfitting. We note that when working with a transformed system, the intrusive ROM approach is usually not viable because it would require rewriting existing code in the transformed variables. In Fig. 1, the intrusive ROM convergence levels off due to differences between the specific volume and conservative variable representations that arise when the PDE is discretized.

B. Continuously Variable Resonance Combustor

The CVRC equations (Eq. 12) are simulated with a heat release parameter of $\alpha = 3.1$ and $\gamma = 1.1756$. At the beginning of the simulation, a small pressure disturbance is applied at the inlet to excite unstable oscillations. The velocity and pressure at the CVRC inlet over the simulation period are shown in Fig. 2a. The POD energy spectrum of the CVRC data is shown in Fig. 2b, and suggests that $r = 10$ basis functions should be sufficient to capture the CVRC behavior.

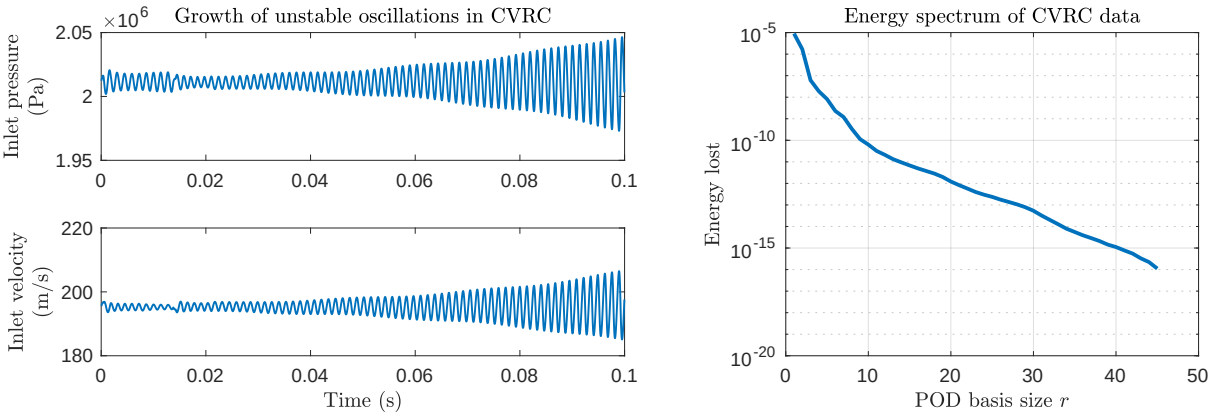

(a) Excitation of combustion instability in CVRC model. A pressure disturbance is applied at the inlet from $t = 0$ to $t = 0.0138$. Subsequent growth of oscillations is self-excited.

(b) POD energy spectrum of CVRC data. With $r = 10$ basis functions we contain all but 10^{-10} of the energy.

Fig. 2 CVRC combustion instability and data energy spectrum.

We process the data to remove the initial transient resulting from the pressure disturbance. We then apply our Transform & Learn framework to the CVRC data using 10 POD basis functions for the transformed state. Fig. 3 shows the Transform & Learn reconstruction of the FOM pressure signature. The qualitative match is excellent, and both the

oscillation frequency and growth rate, two features of particular interest in unstable combustion problems, are matched well. The overall relative state error of the reconstruction is less than 1%.

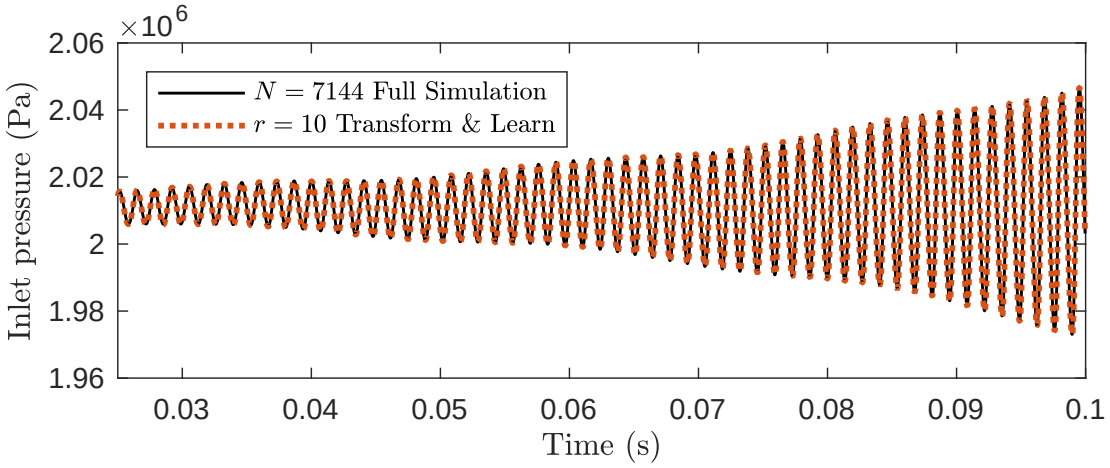

Fig. 3 Transform & Learn ROM reconstruction of CVRC pressure signature.

VI. Conclusions

We have introduced a new method for learning surrogate models for nonlinear PDEs. Our method is based on the identification of a variable transformation in which the PDE for the transformed state has linear-quadratic structure. We give examples of such transformations, which exist for many fluid dynamics applications. We evaluate existing codes to obtain state and time derivative data in the original variables and transform these data to the new state representation in order to formulate a structured model learning problem. The transformed data are projected onto a basis of smaller dimension in order to learn structured reduced-order models.

The accuracy of the learned models is demonstrated on two example problems: the Euler equations and a simple model of a liquid-fueled rocket combustor. For the Euler equations, the learned low-dimensional model can reconstruct trajectories from the training set with less than 0.01% error. For the combustor example, the learned model accurately predicts the growth and frequency of oscillations within the combustor with less than 1% error. For the Euler example, our numerical experiments also demonstrate the ability of the learned models to generalize outside their training data sets: when the reduced basis is rich enough, the learned model is able to reconstruct Euler equation trajectories in the test set with less than 0.05% error. For smaller basis sizes, our results demonstrate that the success of the learned model depends critically on the richness of the data and the resultant reduced basis. In future work, we will extend our method to lifting transformations, which introduce auxiliary variables in order achieve quadratic structure.

Acknowledgments

E. Qian thanks the National Science Foundation Graduate Research Fellowship Program and the Fannie and John Hertz Foundation for their support. The authors also acknowledge the support of the Air Force Center of Excellence on Multi-Fidelity Modeling of Rocket Combustor Dynamics (FA9550-17-1-0195), and the U.S. Department of Energy Applied Mathematics Program (DiaMonD Multifaceted Mathematics Integrated Capability Center, DE-FG02-08ER2585, DE-SC0009297). The authors also thank J. Xu and C. Huang for sharing their implementation of the CVRC model.

References

[1] Antoulas, A. C., *Approximation of large-scale dynamical systems*, Vol. 6, SIAM, 2005.

[2] Benner, P., Gugercin, S., and Willcox, K., "A Survey of Projection-Based Model Reduction Methods for Parametric Dynamical Systems," *SIAM Review*, Vol. 57, No. 4, 2015, pp. 483–531.

[3] Kramer, B., and Willcox, K. E., "Nonlinear Model Order Reduction via Lifting Transformations and Proper Orthogonal Decomposition," *AIAA Journal*, 2019. doi:10.2514/1.J057791.

[4] Benner, P., and Breiten, T., "Two-sided projection methods for nonlinear model order reduction," *SIAM Journal on Scientific Computing*, Vol. 37, No. 2, 2015, pp. B239–B260.

[5] Graham, W., Peraire, J., and Tang, K., "Optimal control of vortex shedding using low-order models. Part I—open-loop model development," *International Journal for Numerical Methods in Engineering*, Vol. 44, No. 7, 1999, pp. 945–972.

[6] Tröltzsch, F., and Volkwein, S., "POD a-posteriori error estimates for linear-quadratic optimal control problems," *Computational Optimization and Applications*, Vol. 44, No. 1, 2009, p. 83.

[7] Hesthaven, J. S., Rozza, G., and Stamm, B., *Certified reduced basis methods for parametrized partial differential equations*, Springer, 2016.

[8] Grepl, M. A., Maday, Y., Nguyen, N. C., and Patera, A. T., "Efficient Reduced-Basis Treatment of Nonaffine and Nonlinear Partial Differential Equations," *ESAIM: Mathematical Modelling and Numerical Analysis*, Vol. 41, No. 3, 2007, pp. 575–605.

[9] Veroy, K., Rovas, D. V., and Patera, A. T., "A posteriori error estimation for reduced-basis approximation of parametrized elliptic coercive partial differential equations: 'convex inverse' bound conditioners," *ESAIM: Control, Optimisation and Calculus of Variations*, Vol. 8, 2002, pp. 1007–1028.

[10] Chaturantabut, S., and Sorensen, D., "Nonlinear Model Reduction via Discrete Empirical Interpolation," *SIAM Journal on Scientific Computing*, Vol. 32, No. 5, 2010, pp. 2737–2764.

[11] Astrid, P., Weiland, S., Willcox, K., and Backx, T., "Missing Point Estimation in Models described by Proper Orthogonal Decomposition," *IEEE Transactions on Automatic Control*, Vol. 53, No. 10, 2008, pp. 2237–2251.

[12] Barrault, M., Maday, Y., Nguyen, N. C., and Patera, A. T., "An Empirical Interpolation Method: Application to Efficient Reduced-Basis Discretization of Partial Differential Equations," *Comptes Rendus Mathematique*, Vol. 339, No. 9, 2004, pp. 667–672.

[13] Carlberg, K., Farhat, C., Cortial, J., and Amsallem, D., "The GNAT Method for Nonlinear Model Reduction: Effective Implementation and Application to Computational Fluid Dynamics and Turbulent Flows," *Journal of Computational Physics*, Vol. 242, 2013, pp. 623–647.

[14] Nguyen, N., Patera, A., and Peraire, J., "A Best Points Interpolation Method for Efficient Approximation of Parametrized Functions," *International Journal for Numerical Methods in Engineering*, Vol. 73, No. 4, 2008, pp. 521–543.

[15] Drmac, Z., and Gugercin, S., "A new selection operator for the discrete empirical interpolation method—improved a priori error bound and extensions," *SIAM Journal on Scientific Computing*, Vol. 38, No. 2, 2016, pp. A631–A648.

[16] Huang, C., Xu, J., Duraisamy, K., and Merkle, C., "Exploration of Reduced-Order Models for Rocket Combustion Applications," *2018 AIAA Aerospace Sciences Meeting*, 2018, p. 1183.

[17] Bergmann, M., Bruneau, C., and Iollo, A., "Enablers for robust POD models," *Journal of Computational Physics*, Vol. 228, No. 2, 2009, pp. 516–538.

[18] Kutz, J. N., Proctor, J., and Brunton, S., "Applied Koopman Theory for Partial Differential Equations and Data-Driven Modeling of Spatio-Temporal Systems," *Complexity*, Vol. 2018, 2018.

[19] Brunton, S. L., Proctor, J. L., and Kutz, J. N., "Discovering governing equations from data by sparse identification of nonlinear dynamical systems," *Proceedings of the National Academy of Sciences*, 2016, p. 201517384.

[20] Hornik, K., Stinchcombe, M., and White, H., "Multilayer feedforward networks are universal approximators," *Neural networks*, Vol. 2, No. 5, 1989, pp. 359–366.

[21] Swischuk, R., Mainini, L., Peherstorfer, B., and Willcox, K., "Projection-based model reduction: formulations for physics-based machine learning," *Computers and Fluids*, Vol. 179, 2019, pp. 704–717.

[22] Rudy, S. H., Brunton, S. L., Proctor, J. L., and Kutz, J. N., "Data-driven discovery of partial differential equations," *Science Advances*, Vol. 3, No. 4, 2017, p. e1602614.

[23] Schaeffer, H., Tran, G., and Ward, R., "Extracting sparse dynamics from limited data," *SIAM Journal on Applied Mathematics*, Vol. 78, No. 6, 2018, pp. 3279–3295.

[24] Peherstorfer, B., and Willcox, K., "Data-driven operator inference for nonintrusive projection-based model reduction," *Computer Methods in Applied Mechanics and Engineering*, Vol. 306, 2016, pp. 196–215.

[25] Gu, C., "QLMOR: A projection-based nonlinear model order reduction approach using quadratic-linear representation of nonlinear systems," *IEEE Transactions on Computer-Aided Design of Integrated Circuits and Systems,*, Vol. 30, No. 9, 2011, pp. 1307–1320.

[26] Lumley, J. L., "The Structure of Inhomogeneous Turbulent Flows," *Atmospheric Turbulence and Radio Wave Propagation*, 1967.

[27] Sirovich, L., "Turbulence and the Dynamics of Coherent Structures. I-Coherent Structures. II-Symmetries and Transformations. III-Dynamics and Scaling," *Quarterly of Applied Mathematics*, Vol. 45, 1987, pp. 561–571.

[28] Bui-Thanh, T., Damodaran, M., and Willcox, K. E., "Aerodynamic data reconstruction and inverse design using proper orthogonal decomposition," *AIAA Journal*, Vol. 42, No. 8, 2004, pp. 1505–1516.

[29] Tadmor, G., Centuori, M., Lehmann, O., Noack, B., Luctenburg, M., and Morzynski, M., "Low Order Galerkin Models for the Actuated Flow Around 2-D Airfoils," *45th AIAA Aerospace Sciences Meeting and Exhibit*, 2007, p. 1313.

[30] Lieu, T., and Farhat, C., "Adaptation of Aeroelastic Reduced-Order Models and Application to an F-16 Configuration," *AIAA Journal*, Vol. 45, No. 6, 2007, pp. 1244–1257.

[31] Bui-Thanh, T., Willcox, K., and Ghattas, O., "Parametric Reduced-Order Models for Probabilistic Analysis of Unsteady Aerodynamic Applications," *AIAA Journal*, Vol. 46, No. 10, 2008, pp. 2520–2529.

[32] Amsallem, D., Cortial, J., and Farhat, C., "Towards Real-Time Computational-Fluid-Dynamics-Based Aeroelastic Computations using a Database of Reduced-Order Information," *AIAA Journal*, Vol. 48, No. 9, 2010, pp. 2029–2037.

[33] Berger, Z., Low, K., Berry, M., Glauser, M., Kostka, S., Gogineni, S., Cordier, L., and Noack, B., "Reduced Order Models for a High Speed Jet with Time-Resolved PIV," *51st AIAA Aerospace Sciences Meeting including the New Horizons Forum and Aerospace Exposition*, 2013, p. 11.

[34] Brunton, S. L., Rowley, C. W., and Williams, D. R., "Reduced-Order Unsteady Aerodynamic Models at Low Reynolds Numbers," *Journal of Fluid Mechanics*, Vol. 724, 2013, p. 203–233.

[35] Taira, K., Brunton, S. L., Dawson, S. T., Rowley, C. W., Colonius, T., McKeon, B. J., Schmidt, O. T., Gordeyev, S., Theofilis, V., and Ukeiley, L. S., "Modal Analysis of Fluid Flows: An Overview," *AIAA Journal*, 2017, pp. 4013–4041.

[36] Huang, C., Duraisamy, K., and Merkle, C., "Challenges in Reduced Order Modeling of Reacting Flows," *2018 Joint Propulsion Conference*, 2018, p. 4675.

[37] Cole, J. D., "On a quasi-linear parabolic equation occurring in aerodynamics," *Quarterly of Applied Mathematics*, Vol. 9, No. 3, 1951, pp. 225–236.

[38] Hopf, E., "The partial differential equation $u_t + uu_x = \mu_{xx}$," *Communications on Pure and Applied Mathematics*, Vol. 3, No. 3, 1950, pp. 201–230.

[39] Harvazinski, M. E., Huang, C., Sankaran, V., Feldman, T., Anderson, W., Merkle, C., and Talley, D. G., "Combustion instability mechanisms in a pressure-coupled gas-gas coaxial rocket injector," *49th AIAA/ASME/SAE/ASEE Joint PropulsionConference*, 2013, p. 3990.

[40] Miller, K., Sisco, J., Nugent, N., and Anderson, W., "Combustion instability with a single-element swirl injector," *Journal of Propulsion and Power*, Vol. 23, No. 5, 2007, pp. 1102–1112.

[41] Yu, Y. C., Sisco, J. C., Rosen, S., Madhav, A., and Anderson, W. E., "Spontaneous longitudinal combustion instability in a Continuously Variable Resonance Combustor," *Journal of Propulsion and Power*, Vol. 28, No. 5, 2012, pp. 876–887.

[42] Feldman, T., Harvazinski, M., Merkle, C., and Anderson, W., "Comparison between simulation and measurement of self-excited combustion instability," *48th AIAA/ASME/SAE/ASEE Joint Propulsion Conference & Exhibit*, 2012, p. 4088.

[43] Harvazinski, M. E., Anderson, W. E., and Merkle, C. L., "Analysis of self-excited combustion instabilities using two-and three-dimensional simulations," *Journal of Propulsion and Power*, 2013.

[44] Smith, R., Ellis, M., Xia, G., Sankaran, V., Anderson, W., and Merkle, C., "Computational investigation of acoustics and instabilities in a longitudinal-mode rocket combustor," *AIAA Journal*, Vol. 46, No. 11, 2008, pp. 2659–2673.

[45] Smith, R., Xia, G., Anderson, W., and Merkle, C., "Computational studies of the effects of oxidiser injector length on combustion instability," *Combustion Theory and Modelling*, Vol. 16, No. 2, 2012, pp. 341–368.

[46] Frezzotti, M. L., Nasuti, F., Huang, C., Merkle, C., and Anderson, W. E., "Response function modeling in the study of longitudinal combustion instability by a Quasi-1D eulerian solver," *51st AIAA/ASME/SAE/ASEE joint propulsion conference, Orlando, FL, USA*, 2015, pp. 27–29.

[47] Xu, J., and Duraisamy, K., "Reduced-Order Reconstruction of Model Rocket Combustor Flows," *53rd AIAA/SAE/ASEE Joint Propulsion Conference*, Atlanta, GA, 2017, p. 4918. doi:doi:10.2514/6.2017-4918.